ARMY RESEARCH LABORATORY

Penetration of Semi-Infinite, Bi-Element Targets by Long Rod Penetrators

Nevin L. Rupert
Fred I. Grace

ARL-TR-666

January 1995

NOTICES

REPORT DOCUMENTATION PAGE

Form Approved
OMB No. 0704-0188

1. AGENCY USE ONLY (Leave blank)	2. REPORT DATE	3. REPORT TYPE AND DATES COVERED
	January 1995	Final, 1 Oct 92–30 Sep 93

4. TITLE AND SUBTITLE
Penetration of Semi-Infinite, Bi-Element Targets by Long Rod Penetrators

5. FUNDING NUMBERS
PR: 1L162618AH80

6. AUTHOR(S)
Nevin L. Rupert and Fred I. Grace

7. PERFORMING ORGANIZATION NAME(S) AND ADDRESS(ES)
U.S. Army Research Laboratory
ATTN: AMSRL-WT-TA
Aberdeen Proving Ground, MD 21005-5066

8. PERFORMING ORGANIZATION REPORT NUMBER -

9. SPONSORING/MONITORING AGENCY NAME(S) AND ADDRESS(ES)
U.S. Army Research Laboratory
ATTN: AMSRL-OP-AP-L
Aberdeen Proving Ground, MD 21005-5066

10. SPONSORING/MONITORING AGENCY REPORT NUMBER
ARL-TR-666

11. SUPPLEMENTARY NOTES

12a. DISTRIBUTION/AVAILABILITY STATEMENT
Approved for public release, distribution is unlimited.

12b. DISTRIBUTION CODE

13. ABSTRACT *(Maximum 200 words)*

The use of semi-infinite, bi-element targets arises from the previous development of the depth of penetration (DOP) testing for ranking ceramic materials. Performance is measured by the DOP of a long rod penetrator into a semi-infinite steel backplate after passing through a ceramic applique. Here, an additional step was taken before evaluating a ceramic applique. Metallic bi-element targets were tested to identify possible nonmaterial-related effects present in DOP testing. As a result, this work identifies and postulates a dynamic effect inherent in both metal/metal and ceramic/metal bi-element targets, establishing a clear separation between kinematic effects and ceramic responses.

14. SUBJECT TERMS
ballistics, depth of penetration, armor, ceramics, dynamic effect

15. NUMBER OF PAGES 31

16. PRICE CODE

17. SECURITY CLASSIFICATION OF REPORT	18. SECURITY CLASSIFICATION OF THIS PAGE	19. SECURITY CLASSIFICATION OF ABSTRACT	20. LIMITATION OF ABSTRACT
UNCLASSIFIED	UNCLASSIFIED	UNCLASSIFIED	UL

INTENTIONALLY LEFT BLANK.

ACKNOWLEDGMENTS

The authors wish to thank Mr. Konrad Frank for his counsel and his assistance in providing the Alekseevkii and Tate calculations and Mr. Stephan R. Bilyk for the CTH hydrocode calculations. Also, appreciation is given to Mr. Matthew Burkins and Mr. Steven Boyer for their support in conducting the depth of penetration (DOP) tests.

INTENTIONALLY LEFT BLANK.

TABLE OF CONTENTS

INTENTIONALLY LEFT BLANK.

LIST OF FIGURES

LIST OF TABLES

INTENTIONALLY LEFT BLANK.

1. INTRODUCTION

The use of semi-infinite, bi-element targets arises from the development of the depth of penetration (DOP) testing for ranking ceramic materials (Woolsey, Mariano, and Kokidko 1989; Alme and Bless 1989a, 1989b; Bless, Rosenberger, and Yoon 1987; Woolsey, Mariano, and Kokidko 1990; Woolsey 1991, 1992). Performance is measured by the DOP of a long rod penetrator into a semi-infinite steel backplate after passing through a ceramic applique. The penetrator velocity is held constant while the areal density/thickness of the ceramic is varied over a wide range of values. The resulting performance maps are then used to compare ceramic performance.

This test method has proven to be a valuable tool for comparative testing and ranking of ceramics. However, little work has been done to exploit this test procedure in conjunction with computational analysis to improve constitutive models. In this study, the evaluation of the bi-element targets followed a two-step procedure. First, a series of metallic bi-element targets was tested and modeled to determine the effectiveness of the computational models and determine target configuration effects. Second, a baseline ceramic was considered and modeled to establish the characteristic ceramic response in DOP testing for comparison with the metallic bi-element targets. This approach has resulted in the identification of a dynamic effect referred to as the density effect mechanism for both metallic and ceramic appliques (Rupert and Grace 1993). It also demonstrates the usefulness of the present approach in studying bi-element armors.

2. MATERIALS

2.1 Steel. Standard U.S. Army practice calls for using armor performance measures in terms of mass- and space-efficiency factors, E_m and E_s, that are defined in terms of a reference steel (for example, rolled homogeneous armor [RHA] [Frank 1981]). The military specifications for the manufacturing process and material properties of RHA are described in MIL-A-12560G(MR) (U.S. Army Materials and Mechanics Research Center 1984). Typical room temperature property data for RHA were measured from random 100- to 152-mm RHA plates used at the Ballistic Research Laboratory (now a part of the Army Research Laboratory) over the past 10 years and are listed in Table 1.

2.2 Titanium. Since the introduction of titanium and titanium alloys in the early 1950s, these materials have in a relatively short time become the backbone materials for the aerospace, energy, and

Table 1. Property Data

	RHA Steel (MIL-A-12560)	Titanium (6A1/4V)	Alumina[a]
Density	7.85 g/cm^3	4.45 g/cm^3	3.895 g/cm^3
% Theoretical Density	N/A	N/A	97.7
Hardness (BHN)	241-375	302-340	12.6 GPa[b]
Crystal Size[c] (Range)	N/M	N/M	1–20 Microns
(Average)	N/M	N/M	2.5–4 Microns
Compressive Strength	N/M	N/M	2,785 MPa
Tensile Strength	793–1,172 MPa	896–910 MPa	262 MPa
Yield Strength	655–1,055 MPa	827–862 MPa	N/A
% Elongation	8–20	10–12	N/A
Young's Modulus	207 GPa	113.8 GPa	383 GPa
Poisson's Ratio	0.29	0.342	0.23
Sonic Velocity	5,876 m/s	6,070 m/s	10.7 km/s

N/A - not applicable.
N/M - not measured.
[a] Coors Ceramic Company, undated.
[b] Knoop 1,000 G.
[c] Measured from polished sections.

chemical industries (Bomberger, Froes, and Morton 1985). The combination of high strength-to-weight ratio, excellent mechanical properties (i.e., strength vs. temperature), and corrosion resistance makes titanium the best material for many critical applications. However, the traditional high cost of titanium alloys has limited their use to applications for which lower cost materials, such as aluminum and steel, could not be used.

Ti-6Al-4V alloy dominates structural casting applications. This alloy similarly has dominated wrought industry products since its introduction in the early 1950s, becoming the benchmark alloy against which others are compared (Eylon, Newman, and Thorne 1990). With the recent reduction in the cost of titanium alloys, a renewed interest in using titanium as an armor material is taking place. Property data measured from armor plates used in the recent evaluation of low-cost Ti-6Al-4V plates are listed in Table 1.

2.3 Alumina (99.5%) Baseline. Reference ceramics are used to develop standards against which other ceramics may be compared. AD-995 Alumina from Coors Ceramic Company has been selected as the baseline for DOP testing using a length-to-diameter (L/D) ratio of 10 for a depleted uranium (DU) 65-g penetrator.

The Coors AD-995 Alumina is a sintered aluminum oxide (Al_2O_3). These tiles were nominally 99.5% pure, 152-mm (6 in) square tiles with thicknesses ranging from 10 mm to 50 mm. Additional property data are listed in Table 1.

3. DOP TESTING

DOP testing was developed as a means of ranking ceramic materials for ballistic applications (Woolsey, Mariano, and Kokidko 1989; Alme and Bless 1989a, 1989b; Bless, Rosenberger, and Yoon 1987; Woolsey, Mariano, and Kokidko 1990). Performance is measured by the DOP of a long rod penetrator into a semi-infinite steel backplate after passing through a ceramic applique. Ceramic performance comparisons are then made between selected baseline ceramic materials. We have extended this type of testing to include bi-element metallic targets.

With this study's use of multi-material laminated target designs, certain implied assumptions are required when calculating E_m and E_s. These assumptions include the following: (1) Elemental e_m and e_s are additive. There are no interactions or synergistic effects associated with the bi-element target; (2) The elemental e_m and e_s of the rear element are constants, and independent of the residual penetrator length and velocity at the interface between the two elements; (3) Velocity corrections for calculating E_m and E_s are equivalent to velocity corrections for a semi-infinite target of the rear element.

3.1 <u>Projectiles</u>. The projectile used in this study was the 65-g, U-0.75% titanium, long rod penetrator manufactured by Nuclear Metals, Incorporated. The penetrator had a diameter of 7.70 mm, and an L/D of 10. Nominal material properties for these penetrators are as follows: density - 18.6 g/cm^3, hardness - R_c 38–44, yield strength - 800 MPa, ultimate strength - 1,380 MPa, and elongation - 12% (Leonard, Magness, and Kapoor 1992).

3.2 <u>Range Setup</u>. The penetrators were fired from a laboratory gun consisting of a 37-mm gun breech assembly with a custom-made 26-mm smoothbore barrel. The gun was positioned approximately 3 m in front of the targets. High-speed (flash) radiography was used to record and measure projectile pitch and velocity. Two pairs of orthogonal x-ray tubes were positioned in the vertical and horizontal planes along the shot line, as illustrated in Figure 1. Propellant weight was adjusted for desired nominal velocity of 1,500 m/s. Projectiles with striking total yaws in excess of 2° were considered "no tests," and those data were disregarded.

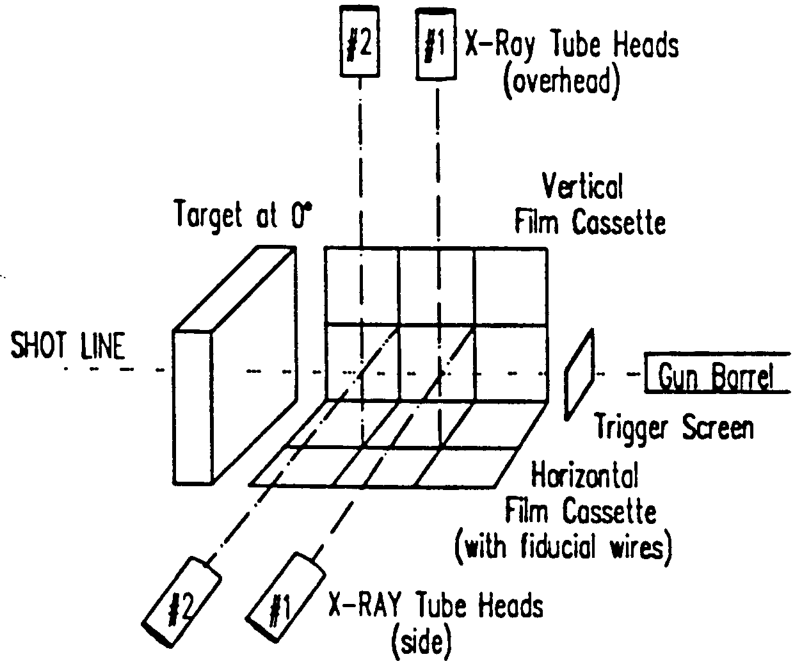

Figure 1. Test setup.

3.3 Target Construction.

3.3.1 All Metal DOP Target Construction. Metal targets were multi-hit targets nominally 152.2 mm × 304.4 mm (6 in × 12 in) in size. The first element consisted of a single plate mechanically clamped to the second element. The second element construction varied with the material used. RHA second elements were 127-mm (5 in)-thick, MIL-A-12560, Class 3 steel plates. Titanium second elements were 101.6-mm (4 in)-thick, Ti-6Al-4V alloy.

3.3.2 Al_2O_3 DOP Target Construction. Target construction followed the standard design as shown in Figure 2 (Woolsey, Mariano, and Kokidko 1989; Woolsey, Mariano, and Kokidko 1990; Woolsey 1991, 1992). This design consisted of either a 101.6-mm (4 in) or a 152.4-mm (6 in)-square ceramic tile held into a steel lateral confinement frame by EPON 828 and VERSAMID 140, with a mixing ratio of 1:1. The frame has a 19-mm (3/4 in) web, and a depth equal to or greater than the tile thickness. The frame is then mechanically clamped to a thick steel backup plate. This backup plate is RHA steel, MIL-A-12560, Class 3, 127 mm (5 in) thick, with a nominal hardness of R_c 27.

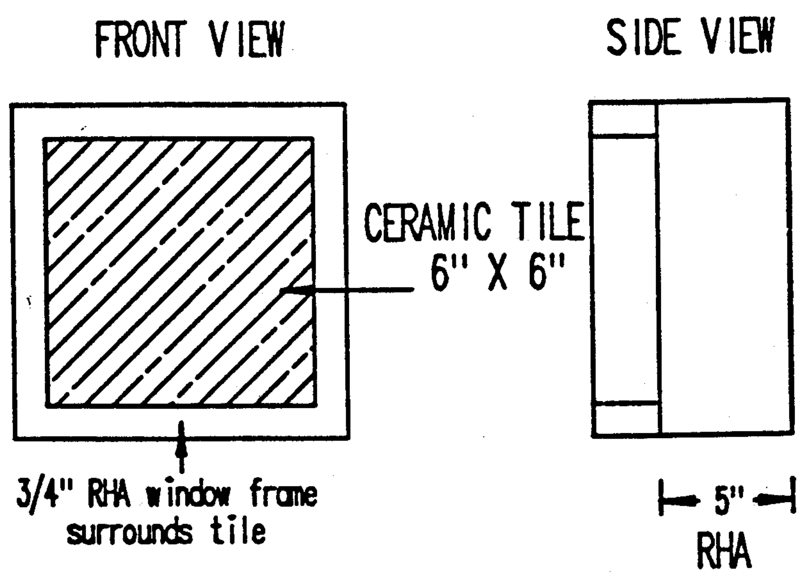

Figure 2. DOP ceramic target.

4. TEST RESULTS

4.1 Monolithic RHA Data. Monolithic penetration data for the DU penetrator used in this test series are available over a wide range of velocities, from 700 m/s to 1,800 m/s. Over this range of interest, the data are linear, and a regression fit to the penetration data was derived for RHA steel. The resulting equation is as follows:

$$DOP = 0.068\,V_s - 27.2, \tag{1}$$

where V_s is the striking velocity in meters/second, while DOP and the right-hand constant are in millimeters (see Figure 3). In order to correct for variations in the actual striking velocities, all residual penetration values for ceramic and metallic bi-element targets were normalized to a striking velocity of 1,500 m/s by the following correction based on equation (1):

$$DOP' = \text{Measured DOP} + 102 - 0.068V_s. \tag{2}$$

This technique should be uniformly valid for different materials if a significant amount of the rod reaches the RHA steel backplate (Woolsey, Mariano, and Kokidko 1990).

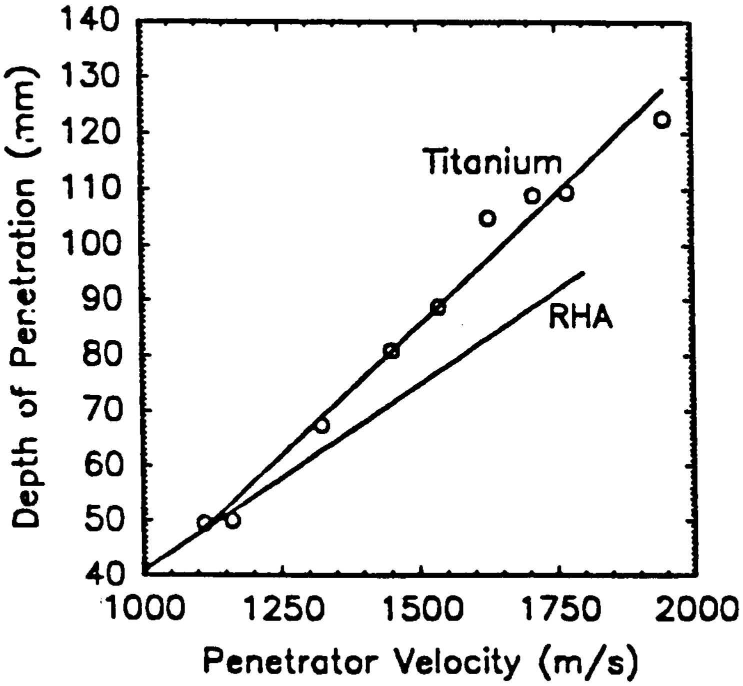

Figure 3. Baseline metallic data.

4.2 Monolithic Titanium Data. Monolithic Ti-6Al-4V penetration data against the DU penetrator are based on nine tests ranging from 1,100 m/s to 1,950 m/s (see Figure 3) (Burkins 1991). Over this range, the data are linear, and a regression fit to the data was derived. The resulting equation is as follows:

$$DOP_{(Ti)} = 0.0949\, V_s - 56.7, \tag{3}$$

where V_s is the striking velocity in meters/second, and the DOP and constant are in millimeters. In order to correct for variations in the actual striking velocities, all residual penetration values for metallic bi-element targets will be normalized to a striking velocity of 1,500 m/s by the following correction based on equation (3):

$$DOP'_{(Ti)} = \text{Measured}\, DOP_{(Ti)} + 142 - 0.0949\, V_s. \tag{4}$$

4.3 Titanium/Steel Data. Average corrected DOP results for the 12 titanium/RHA bi-element targets are shown in Figure 4 and listed in Appendix A. The open circles plot the individual data points for the bi-element targets. The solid line represents a regression fit to the corrected DOP results, excluding the semi-infinite end points. Corrections for velocity fluctuations were generally less than 2 mm. The solid circles in Figure 4 represent the semi-infinite data points for both metals. The straight dotted line connecting them represents the expected results from the rule of mixtures based on the assumptions used to calculate E_m and E_s. This line is defined in equation (5):

$$DOP = DOP_{(2)} * \left[1 - \frac{T_{(a)}}{DOP_{(1)}} \right] , \tag{5}$$

where $DOP_{(2)}$ is the semi-infinite DOP value for the second element, $DOP_{(1)}$ is the semi-infinite DOP value for the first element, and $T_{(a)}$ is the applique thickness.

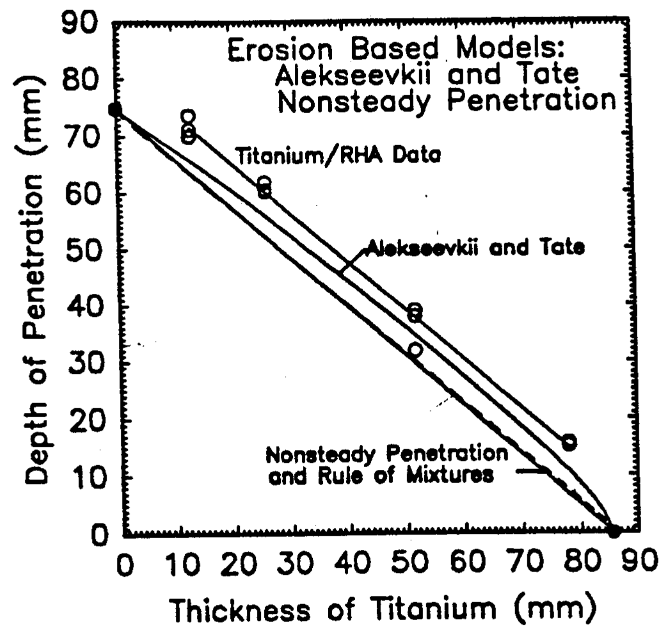

Figure 4. Corrected titanium/RHA data.

There is a substantial difference between the regression curve for the ballistic data and the rule of mixtures curve as the experimental data are shifted up and to the right. An additional effect has occurred from the interaction between the two target elements. In DOP testing of ceramics, the initial shift in the performance plot has been attributed to the lack of dynamic strength and transient effects associated with starting the penetration process. However, these titanium/steel targets demonstrate the same initial shift in the performance map when there is no loss of strength associated with relatively thin metal plates, and no indication of brittle failure. If transient effects caused the shift in the performance map, the effect is thought to lessen as the front plate becomes thicker and to eventually merge with the rule of mixtures as the effect dissipates. Since the DOP performance map shows two parallel lines, transient effects alone cannot fully account for the shift in the penetration results.

Figure 4 also depicts two one-dimensional erosion models used to determine if the shift in the DOP results could be the result of basic characteristics of the target and penetrator. These basic characteristics include such things as the penetrator density and strength, target density and strength, penetrator velocity, penetrator length, and interface velocity. The nonequilibrium enhanced Frank/Zook modified Alekseevkii and Tate model (Frank and Zook 1990) indicated a gradual increase in DOP results over the rule of mixtures as the applique thickness increased. The nonsteady penetration model (Grace and Rupert 1993; Grace 1993) predicted DOP results more closely related to the rule of mixtures. Both models, in their present form, do not fully account for the observed data. Material properties as supplied by the modelers are provided in Table 2.

Table 2. Computational Values

	Grace Model	Frank - Zook Model
RHA	$\rho = 7.85$ g/cm^3 $S_t = 0.91$ GPa c = 6,070 m/s	B = 270 H = 5.0 GPa $K_p = K_t = ½$
Ti-6Al-4V	$\rho = 4.45$ g/cm^3 $S_t = 1.06$ GPa c = 5,876 m/s	B = 330 H = 4.88 GPa $K_p = K_t = ½$

Using the nonsteady penetration model, a series of "what if" calculations was performed in trying to identify possible causes of the shift in the DOP results. Based on these calculations, it was inferred that the unidentified mechanism could be the result of a dynamic target interaction, rather than a material response. DOP results for the 12.8-mm titanium applique were duplicated when the penetration velocity was artifically augmented while penetrating the titanium applique. This resulted in a lower penetrator erosion rate through the titanium applique but did not otherwise alter any of the basic penetrator and target characteristics in the model. This increased the uneroded rod length that arrives at the bi-element target interface, and consequently resulted in higher DOP results into the second element.

4.4 Steel/Titanium Data. Average corrected DOP results for the RHA/titanium bi-element targets are shown in Figure 5 and listed in Appendix B. Examination of the regression curve for the ballistic data and the rule of mixtures curve shows less of an interaction between the two target elements. The ballistic data are statistically less than the rule of mixtures for the 19.5-mm and 39.2-mm RHA applique thicknesses. The most striking aspect of this data is the change in the direction of the shift in the DOP results with respect to the rule of mixtures as a result of reversing the order of the materials.

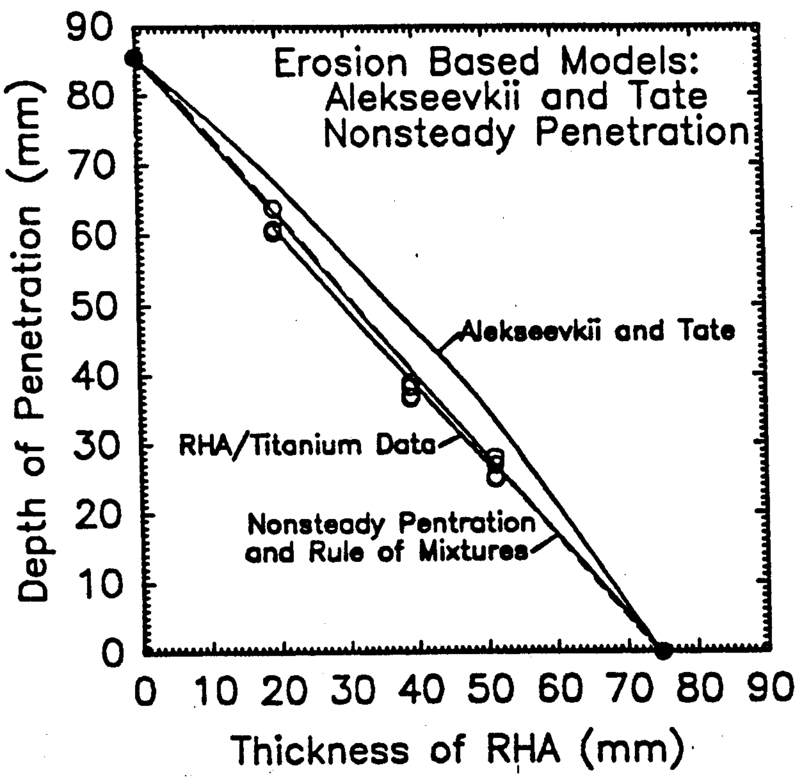

Figure 5. Corrected RHA/titanium data.

The two one-dimensional erosion models were used again to determine if reversal in the shift of the DOP results is related to the basic characteristics of the target and penetrator or the unidentified mechanism. The nonequilibrium, enhanced Frank/Zook modified Alekseevkii and Tate model again indicated a gradual increase in the DOP results as the applique thickness increased. The nonsteady penetration model again predicted DOP results closely related to the rule of mixtures. Both models showed no bias as to the order of the metals in their prediction of the DOP results. Aside from the modeling, the physical property data observations show that reversing material order does not reverse the strength order of the materials involved. However, the material reversal does significantly reverse the densities. This leads to the second inference about the unidentified mechanism; it appears to be density driven.

The differences in densities between elements can create a dynamic target interaction effect under conditions of impact. Although the principles for such interaction are well understood from impact mechanics or shock-wave physics, application to this problem may have been generally overlooked. During impact, pressure or stress waves generated are reflected by the bi-element interface as returning pressure or relief waves, depending on the relative densities, shock impedance and acoustic impedance. However, the steel/titanium target represented a combination of material properties where the acoustic and shock impedance were similar enough to reduce to the difference in densities alone. Thus, a pressure wave reflecting from a higher density second element, and its associated material particle velocity, moves back toward the penetrator. This motion enhances the penetration rate in the first element with corresponding reduction in penetrator erosion rate. Thus, a greater uneroded rod length reaches the bi-element interface, which produces greater DOP into the second element. When the second element has the lower density, an opposite condition exists. The relief wave moves material away from the penetrator, lowers penetration rates, increases rod erosion rates, and lowers uneroded rod length. In that case, DOP into the second element is expected to be somewhat lower.

In a sense, when the second element has the higher density, it acts as an anvil until the first element is sufficiently thick enough to appear semi-infinite. As an overall effect, the interaction can be thought of as an "inertial effect" developed by reflected pressure pulses from the higher density second target element. The amount of change in penetration rate diminishes with increased thickness of the first element. The effect disappears completely as the first element becomes sufficiently thick to appear semi-infinite.

Additional evidential support for this description of the density effect was attained from the use of the Eulerian hydrocode, CTH, public domain version November 1992. The CTH hydrocode was used to simulate the impact of the 65-g DU penetrator into four targets (monolithic titanium, 12.8-mm titanium/RHA, monolithic RHA, and 19.04-mm RHA/titanium) using the Cray-2 supercomputer located at the U.S. Army Research Laboratory, Aberdeen Proving Ground, MD. In all cases, a three-dimensional simulation was performed using an axisymmetric coordinate system, a uniform grid, and 0.77-mm cell size for the first 25 cells, followed by a 2.5% cell expansion in the semi-infinite azimuthal direction. Typically, the radial and axial boundaries of the target were placed approximately 5 penetrator diameters from the impact point. Transmissive boundary conditions were used at the radial and axial edges of the mesh. A set of Lagrangian tracer particles was embedded on the penetrator and target centerline to track various events. The failure mode used was based on user-supplied maximum tensile pressure for each material. When failure occurred, a void was introduced into the material. Material properties used in the computer simulation are listed in Table 3.

Table 3. Computational Property Data

	Depleted Uranium (U-3/4% Ti)	RHA Steel (MIL-A-12560)	Titanium (6A1/4V)
Density	18.95 g/cm^3	7.85 g/cm^3	4.42 g/cm^3
Yield Strength	1,500 MPa	750 MPa	890 MPa
Poisson's Ratio	0.34	0.29	0.34
Sonic Velocity	2,490 m/s	3,570 m/s	5,130 m/s
Gruneisen parameter	1.56	1.69	1.23
U_s-U_p Hugoniot slope	2.20	1.92	1.03

Figures 6–9 are velocity-time plots for the four targets. Lagrangian 1 represents the penetrator/erosion front velocity. Lagrangian 10 represents the penetrator tail velocity. Lagrangian 11 and 12 represent applique interfaces or particles at corresponding depths within monolithic targets. Lagrangian 11 is located at 12.8 mm from the front surface. Lagrangian 12 is 19.04 mm from the front surface. Comparing Figures 6 and 7, the penetrator tail velocities are identical while the penetrator is in the applique. The titanium applique rear surface velocity and acceleration are less than the velocity and acceleration expected for monolithic titanium as shown by comparing the Lagrangian 11 plots. This difference in velocities for the two Lagrangian 11 plots can be the "inertial effect" developed by reflected compressive pressure pulse from the higher density second target element. The initial transient for the erosion front is identical for both the titanium applique and monolithic material. Between 5 µs and 10 µs, a transition region in the curve develops and ends in about 40 µs when the applique is perforated. Comparing Figures 7 and 8 after the applique has been perforated, the remaining velocities for the penetrator's front and tail are identical for both the monolithic RHA and the RHA second element, except for a slight time shift.

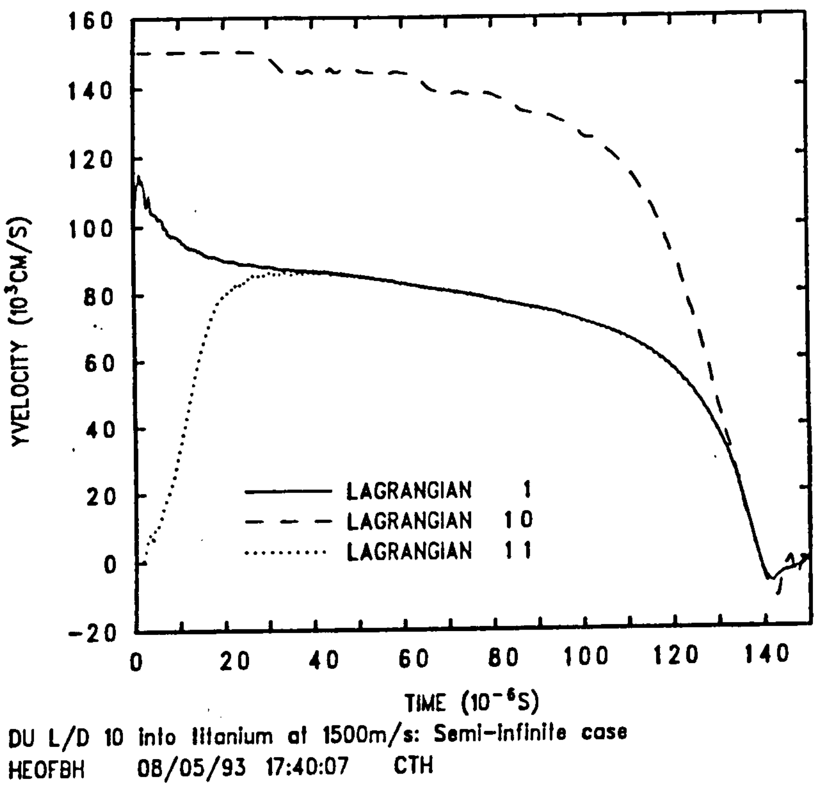

Figure 6. Semi-infinite titanium.

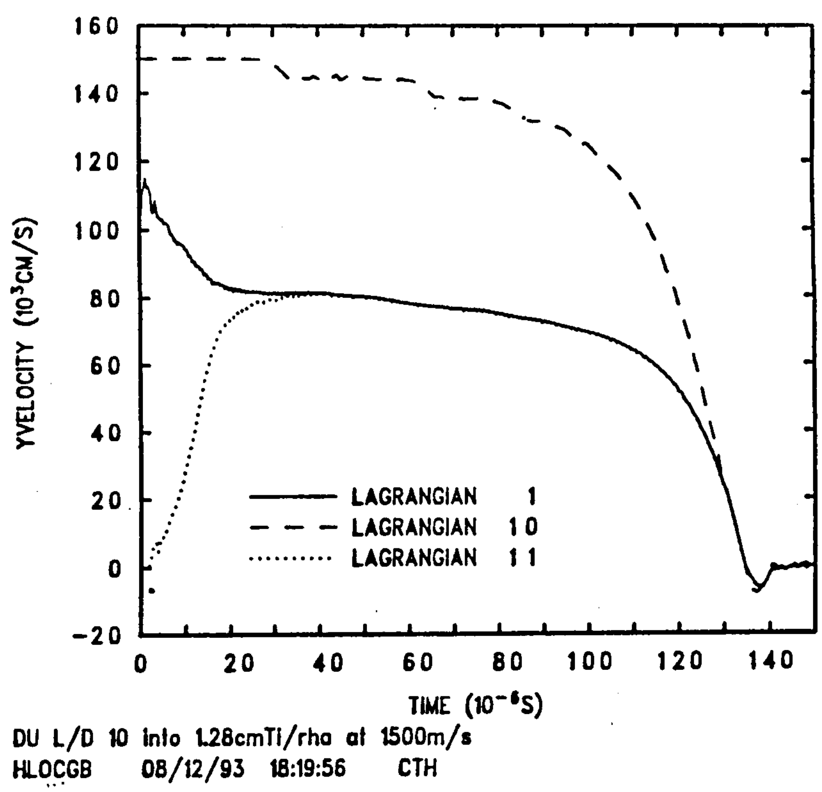

Figure 7. 1.28-cm titanium/RHA.

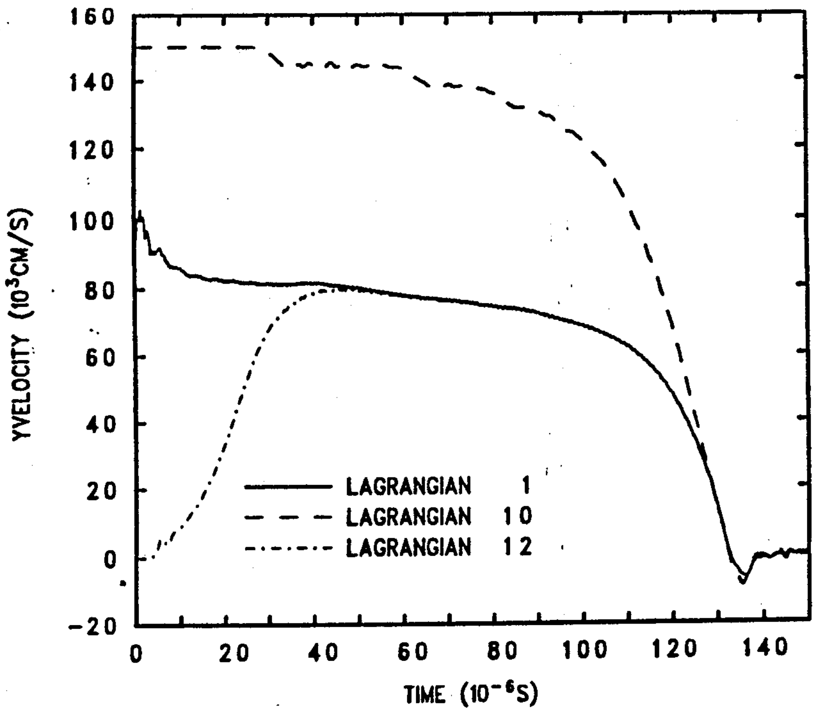

DU L/D 10 into rha at 1500m/s: Semi-infinite case
HDPBVB 08/04/93 17:07:35 CTH

Figure 8. Semi-infinite RHA.

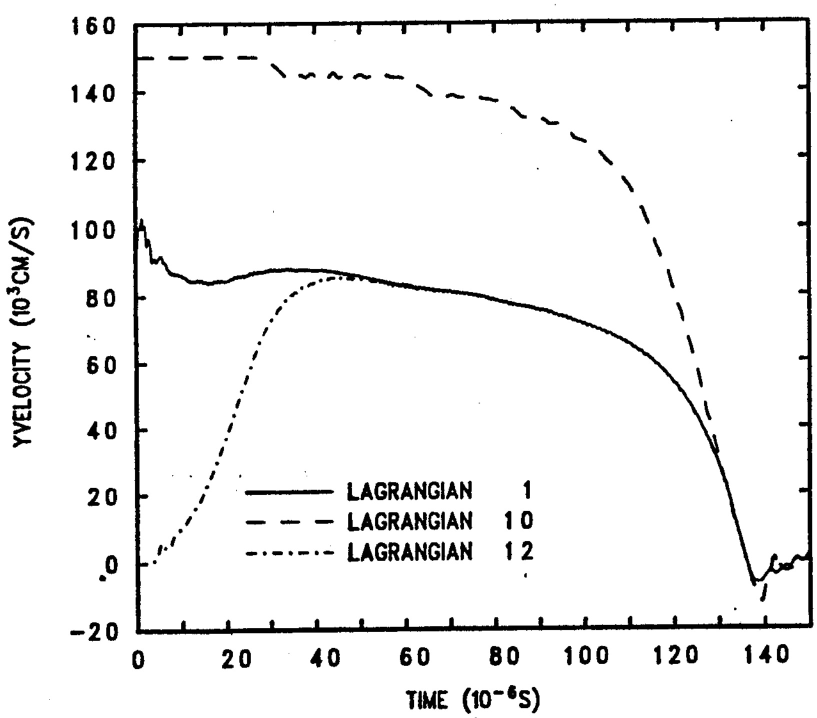

DU L/D 10 into 1.90cm RHA/Ti at 1500m/s
HZSCYZ 08/26/93 22:07:19 CTH

Figure 9. 1.904-cm RHA/Ti.

Comparing Figures 8 and 9, the penetrator tail velocities are again identical while the penetrator is in the applique. The RHA applique rear surface velocity and acceleration are greater than the velocity and acceleration expected based on the monolithic RHA calculations. This difference in velocities for the two Lagrangian 12 plots is the expected reversal resulting from the "inertial effect." The reflected pressure pulse from the lower density second target element into the first element has changed from a compressive wave to a tensile wave. Again, between 5 μs and 10 μs, a transition region in the curve develops and ends in about 40 μs when the applique is perforated. Comparing Figures 9 and 6, after the applique has been perforated, the remaining velocities for the penetrator's front and tail are identical for both the monolithic titanium and the titanium second element, except for a slight time shift.

4.5 Al_2O_3/Steel Data. To provide a suitable comparison to other ceramics, the baseline Al_2O_3 targets were fired over a range of ceramic thicknesses/areal densities (Burkins 1991). Results are depicted graphically in Figure 10. Individual data points are represented by open circles on the graph. The solid line is the resulting equation from a first-order regression of the corrected baseline ceramic data. Equation (6) is the mathematical expression for this linear regression:

$$DOP' = 80.0 - 1.315\,T, \tag{6}$$

where T is the thickness of the Al_2O_3 applique, and the quantities are expressed in millimeters. The dotted line represents a fourth-order regression of the corrected DOP results. This regression more closely resembles the generalized performance map for the ceramic (Woolsey, Mariano, and Kokidko 1990) but does not add to the precision of the performance estimates.

In the generalized performance map of DOP data, Woolsey et al. postulated four regions which were thought to correspond to different material responses (Woolsey, Mariano, and Kokidko 1990). In this brief analysis, the discussion will be limited to regions 1 and 2. Region 1 was defined as thickness-affected penetration of the ceramic applique, where failure is rapid due to the low thickness of the tile in relation to the penetrator diameter. Region 2 was defined as when the overmatching of the tile becomes less severe, and significant performance gains are observed. The preceding discussion regarding metallic bi-element targets suggests that the shift in ceramic response in region 1 is the density effect, rather than loss of material strength. Region 2 can then be redefined as the onset of strength degradation due to time-dependent damage within the ceramic applique. Since most ceramics used in ballistic applications are of low density, between 2.5 g/cm^3 and 4.5 g/cm^3, Woolsey, Mariano, and Kokidko's observation that all currently tested ceramics are expected to follow the same trends is not inconsistent with the density effect. However, their contention that region 1 is the resulting material response is inconsistent with the dynamic effect resulting from target configuration as observed in the metallic bi-element targets.

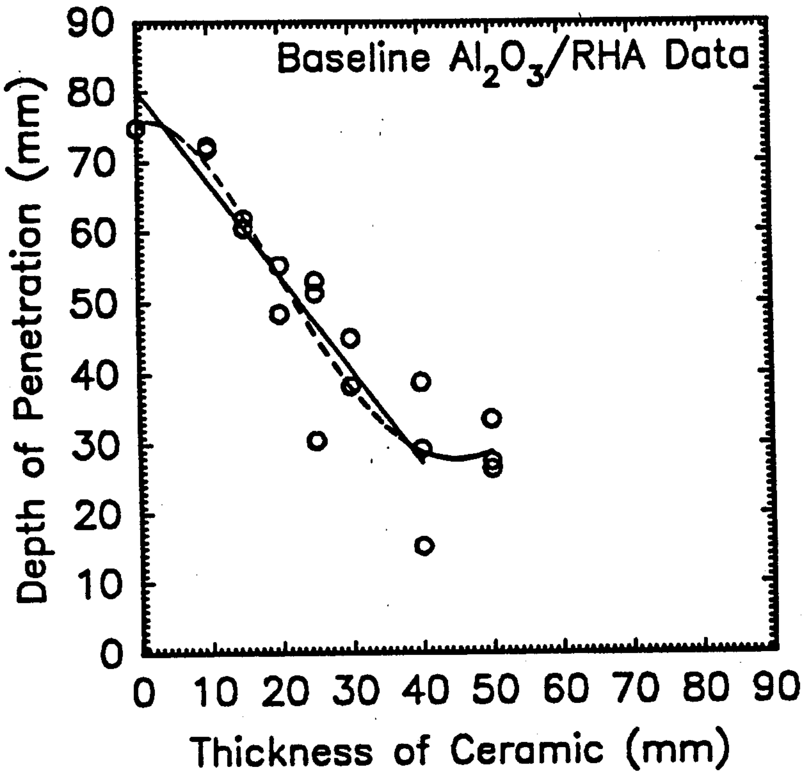

Figure 10. Al_2O_3 data.

5. CONCLUSIONS

This work considers a previously overlooked dynamic target interaction effect that is inherent in both metal/metal bi-element targets.[1] The effect labeled inertial effect or density effect is consistent with impact mechanics and results from the orientation and differences in densities between the two elements. By considering the density effect, a clear separation between dynamic effect and material responses is now possible in DOP testing. This allows an already valuable tool for comparative testing and ranking ceramics to become one that can also aid the development of ceramic constitutive models.

[1] Similar shifts in ceramic/metal bi-element targets may also be explained by this dynamic target interaction.

INTENTIONALLY LEFT BLANK.

6. REFERENCES

Alme, M., and S. J. Bless. "Experiments to Determine the Ballistic Resistance of Confined Ceramics at Hypervelocity." Draft Report for DARPA, September 1988, published in Proceedings of the Fifth TACOM Armor Conference, March 1989.

Alme, M., and S. J. Bless. "Measuring the Ballistic Resistance of Armor Ceramics." ATAC Bullet, 1989.

Bless, S. J., Z. Rosenberger, and B. Yoon. "Hypervelocity Penetration of Ceramics." International Journal of Impact Engineering, vol. 5, pp. 165–171, 1987.

Bomberger, H. B., F. H. Froes, and P. H. Morton. "Titanium—A Historical Perspective." Titanium Technology: Present Status and Future Trends. Edited by F. H. Froes, D. Eylon, and H. B. Bomberger, pp. 3–17, 1985.

Burkins, M. Unpublished Data, U.S. Army Ballistic Research Laboratory, Aberdeen Proving Ground, MD, 1991.

Coors Ceramic Company. "Application Guide." Structural Division, Bulletin No. 980, Boulder, CO, undated.

Eylon, D., J. R. Newman, and J. K. Thorne. "Titanium and Titanium Alloy Casting." Metals Handbook, Properties and Selection: Nonferrous Alloys and Special-Purpose Materials, 10th edition, vol. 2, pp. 634–646, 1990.

Frank, K. "Armor-Penetration Performance Measures." BRL-MR-03097, U. S. Army Ballistic Research Laboratory, Aberdeen Proving Ground, MD, 1981.

Frank, K., and J. Zook. "Chunky Metal Penetrators Act Like Constant Mass Penetrators." Proceedings of the Twelfth International Symposium on Ballistics, vol. 1, pp. 441–449, San Antonio, TX, 30 October–1 November 1990.

Grace, F. I. "Non-Steady Penetration of Long Rods into Semi-Infinite Targets." International Journal of Impact Engineering, vol. 14, pp. 303–314, 1993.

Grace, F. I., and N. L. Rupert. "Mechanisms for Ceramic/Metal, Semi-Infinite, Bi-Element Target Response to Ballistic Impact." TB-16, Ballistics '93, 14th International Symposium, vol. 2, pp. 361–370, Quebec City, Quebec, Canada, 1993.

Leonard, W., L. Magness, Jr., and D. Kapoor. "Ballistic Evaluation of Thermo-Mechanically Processed Tungsten Heavy Alloys." BRL-TR-3326, U.S. Army Ballistic Research Laboratory, Aberdeen Proving Ground, MD, April 1992.

Rupert, N. L., and F. I. Grace. "Penetration of Long Rods Into Semi-Infinite, Bi-Element Targets," TB-27, Ballistics '93, 14th International Symposium, vol. 2, pp. 469–478, Quebec City, Quebec, Canada, 1993.

U.S. Army Materials and Mechanics Research Center. Armor Plate, Steel, Wrought, Homogeneous (for use in Combat-Vehicles and for Ammunition Testing). Military Specification MIL-A-12560G, Watertown, MA, 15 August 1984.

Woolsey, P. "Residual Penetration Ballistic Testing of Armor Ceramics." Second TACOM Combat Vehicle Survivability Symposium, April 1991.

Woolsey, P. "Ceramic Materials Screening by Residual Penetration Testing." Proceedings of the Thirteenth International Ballistic Symposium, June 1992.

Woolsey, P., S. Mariano, and D. Kokidko. "Alternative Test Methodology for Ballistic Performance Ranking of Armor Ceramics." Proceedings of the Fifth TACOM Armor Conference, March 1989.

Woolsey, P., S. Mariano, and D. Kokidko. "Progress Report on Ballistic Test Methodology for Armor Ceramics." Proceedings of the First TACOM Combat Vehicle Survivability Symposium, March 1990.

APPENDIX A:

DEPTH OF PENETRATION (DOP) RESULTS FOR Ti-6Al-4V/RHA

INTENTIONALLY LEFT BLANK.

Table A-1. Depth of Penetration (DOP) Results for Ti-6Al-4V/RHA

Applique Thickness (mm)	Striking Velocity (m/s)	Pitch (deg)	Yaw (deg)	DOP (mm)	Corrected DOP (mm)
12.8	1,455	0	0.75R	68	71
12.8	1,487	1.0U	0.25L	69	70
12.8	1,507	0.5U	0.25R	74	74
25.9	1,508	0.25U	0.50R	61	60
25.9	1,488	0.50U	0	61	62
25.9	1,512	0.25D	0	61	60
51.7	1,501	0	0.50L	38	38
51.7	1,501	0	0.75R	39	39
51.7	1,502	0.75U	0.50R	32	32
78.0	1,520	0.50D	0	17	16
78.0	1,519	1.00U	0.50R	17	16
78.0	1,512	0.50D	0.50R	16	15

INTENTIONALLY LEFT BLANK.

APPENDIX: B

DEPTH OF PENETRATION (DOP) RESULTS FOR RHA/Ti-6Al-4V

INTENTIONALLY LEFT BLANK.

Table B-1. Depth of Penetration (DOP) Results for RHA/Ti-6Al-4V

Applique Thickness (mm)	Striking Velocity (m/s)	Pitch (deg)	Yaw (deg)	Depth of Penetration (mm)	Corrected DOP (mm)
25.9	1,508	0.25U	0.50R	61	60
25.9	1,488	0.50U	0	61	62
25.9	1,512	0.25D	0	61	60
51.7	1,501	0	0.50L	38	38
51.7	1,501	0	0.75R	39	39
51.7	1,502	0.75U	0.50R	32	32
78.0	1,520	0.50D	0	17	15
78.0	1,519	1.00U	0.50R	17	15
78.0	1,512	0.50D	0.50R	16	15

INTENTIONALLY LEFT BLANK.

NO. OF COPIES	ORGANIZATION
2	ADMINISTRATOR ATTN DTIC DDA DEFENSE TECHNICAL INFO CTR CAMERON STATION ALEXANDRIA VA 22304-6145
1	COMMANDER ATTN AMCAM US ARMY MATERIEL COMMAND 5001 EISENHOWER AVE ALEXANDRIA VA 22333-0001
1	DIRECTOR ATTN AMSRL OP SD TA US ARMY RESEARCH LAB 2800 POWDER MILL RD ADELPHI MD 20783-1145
3	DIRECTOR ATTN AMSRL OP SD TL US ARMY RESEARCH LAB 2800 POWDER MILL RD ADELPHI MD 20783-1145
1	DIRECTOR ATTN AMSRL OP SD TP US ARMY RESEARCH LAB 2800 POWDER MILL RD ADELPHI MD 20783-1145
2	COMMANDER ATTN SMCAR TDC US ARMY ARDEC PCTNY ARSNL NJ 07806-5000
1	DIRECTOR ATTN SMCAR CCB TL BENET LABORATORIES ARSENAL STREET WATERVLIET NY 12189-4050
1	DIR USA ADVANCED SYSTEMS ATTN AMSAT R NR MS 219 1 R&A OFC AMES RESEARCH CENTER MOFFETT FLD CA 94035-1000

NO. OF COPIES	ORGANIZATION
1	COMMANDER ATTN AMSMI RD CS R DOC US ARMY MISSILE COMMAND REDSTONE ARSNL AL 35898-5010
1	COMMANDER ATTN AMSTA JSK ARMOR ENG BR US ARMY TANK AUTOMOTIVE CMD WARREN MI 48397-5000
1	DIRECTOR ATTN ATRC WSR USA TRADOC ANALYSIS CMD WSMR NM 88002-5502
1	COMMANDANT ATTN ATSH CD SECURITY MGR US ARMY INFANTRY SCHOOL FT BENNING GA 31905-5660
	ABERDEEN PROVING GROUND
2	DIR USAMSAA ATTN AMXSY D AMXSY MP H COHEN
1	CDR USATECOM ATTN AMSTE TC
1	DIR USAERDEC ATTN SCBRD RT
1	CDR USACBDCOM ATTN AMSCB CII
1	DIR USARL ATTN AMSRL SL I
5	DIR USARL ATTN AMSRL OP AP L

NO. OF COPIES	ORGANIZATION
1	HQDA SARD TT DR F MILTON WASH DC 20310-0103
1	HQDA SARD TT MR J APPEL WASH DC 20310-0103
2	DIR DARPA ATTN JAMES RICHARDSON 3701 N FAIRFAX DR ARLINGTON VA 22203-1714
1	DEFENSE NUCLEAR AGENCY ATTN TECH LIBRARY 6801 TELEGRAPH RD ALEXANDRIA VA 22192
1	CDR US ARMY RSCH OFC ATTN KALISIM LYER PO BOX 12211 4300 MIAMI BLVD RSCH TRI PK NC 27709
2	CDR US ARMY MICOM ATTN AMSMI RD ST WF DONALD LOVELACE MICHAEL SCHEXNAYDER REDSTONE ARSNL AL 35898-5250
1	CDR US ARMY TACOM RD&E CENTER ATTN AMCPM ABMS SA JOHN ROWE WARREN MI 48397-5000
1	CDR US ARMY BELVOIR RD&E CTR ATTN STRBE NAN TECH LIBRARY FT BELVOIR VA 22060-5166
6	CDR US ARMY ARDEC ATTN SMCAR AAE W JAMES PEARSON TECH LIBRARY PCNTY ARSNL NJ 07806-5000
1	PM TANK MAIN ARMNT SYSTEMS ATTN SSAE AR TMA MT PCNTY ARSNL NJ 07806-5000

NO. OF COPIES	ORGANIZATION
1	USMC MCRDAC PM GRNDS WPNS BR ATTN DAN HAYWOOD FIREPOWER DIV QUANTICO VA 22134
1	CH OF NAVAL RSCH OFC OF NAVAL TECH ATTN A J FAULSDITCH ONT 23 BALLSTON TOWERS ARLINGTON VA 22217
1	NAVAL WPNS CTR ATTN TECH LIBRARY CHINA LAKE CA 93555
4	CDR NSWC ATTN J C MONOLO CODE G 34 M SHAMBLEN W HORT TECH LIBRARY DAHLGREN VA 22448-5000
1	DIR NAVAL CIVIL ENGR LAB ATTN J YOUNG CODE L 56 PORT HUENEME CA 93043
4	CDR NSWC ATTN R GARRETT R 12 J FOLTZ R 32 H DEJARNETTE R 32 TECH LIBRARY 10901 NEW HAMPSHIRE AVE SILVER SPRNG MD 20903-5000
1	NUSC NEWPORT ATTN S DICKINSON CODE 8214 NEWPORT RI 02841
2	MSD ENL ATTN W DYESS J FOSTER EGLIN AFB FL 32542-5000
1	AIR FORCE ARMNT LAB ATTN TECH LIBRARY EGLIN AFB FL 32542

NO. OF COPIES	ORGANIZATION
4	DIR SANDIA NATIONAL LABS ATTN M KIPP DIV 1533 R GRAHAM DIV 1551 P YARRINGTON TECH LIBRARY PO BOX 5800 ALBUQUERQUE NM 87185
7	DIR LOS ALAMOS NATIONAL LAB ATTN G E CORT F663 R KARPP MS J960 B HOGAN W GASKILL J CHAPYAK MS G787 S MARSH MS 970 M 6 TECH LIBRARY PO BOX 1663 LOS ALAMOS NM 87545
6	DIR LAWRENCE LIVERMORE NATIONAL LAB ATTN J E REAUGH L 290 M FINGER MS 35 D BAUM M WILKINS M J MURPHY TECH LIBRARY PO BOX 808 LIVERMORE CA 94550
1	ROCKWELL INTL ROCKETDYNE DIV ATTN J MOLDENHAUER 6633 CANOGA AVE HB 23 CANOGA PK CA 91303
1	ALLIED SIGNAL ATTN L LIN PO BOX 31 PETERSBURG VA 23804
1	MCDONNELL DOUGLAS HELICOPTER ATTN L R BIRD MS 543 D216 5000 E MCDOWELL RD MESA AZ 85205

NO. OF COPIES	ORGANIZATION
1	AEROJET PRECISION WPNS DEPT 5131 T W ATTN JOSEPH CARLEONE 1100 HOLLYVALE AZUSA CA 91702
1	PHYSICS INTL ATTN JIM COFFENBERRY 2700 MERCED ST PO BOX 5010 SAN LEANDRO CA 94577
1	BOEING CORP ATTN T M MURRAY MS 84 84 PO BOX 3999 SEATTLE WA 98124
1	NUCLEAR METALS INC ATTN R QUINN 2229 MAIN ST CONCORD MA 01742
3	DYNA EAST CORP ATTN P C CHOU R CICCARELLI W FLIS 3201 ARCH ST PHILADELPHIA PA 19104
1	SOUTHWEST RSCH INST ATTN C ANDERSON PO DRAWER 28255 SAN ANTONIO TX 78228-0255
2	ALLIANT TECHSYSTEMS INC ATTN G R JOHNSON C CANDLAND MN 48 2700 7225 NORTHLAND DR BROOKLYN MN 55428
1	AAI CORP N CONNER DEPT 403 BLDG 100 HUNT VALLEY MD 21030
2	GENERAL RSCH CORP ATTN ALEX CHARTERS TOM MENNA PO BOX 6770 SNTA BRBRA CA 93160-6770

NO. OF COPIES	ORGANIZATION
1	GENERAL DYNAMICS ATTN JAIME CUADROS PO BOX 50 800 MAIL ZONE 601-87 ONTARIO CA 91761-1085
1	S CUBED ATTN R SEDGWICK PO BOX 1620 LA JOLLA CA 92038-1620
2	CA RSCH & TECH CORP ATTN ROBERT BROWN DENNIS ORPHAL 5117 JOHNSON DR PLEASONTON CA 94566
2	ORLANDO TECH INC ATTN D MATUSKA J OSBORN PO BOX 855 SHALIMAR FL 32579
1	KAMAN SCIENCES CORP ATTN D BARNETTE PO BOX 7463 CO SPRINGS CO 80933-7463
1	LIVERMORE SOFTWARE TECH CORP ATTN JOHN O HALLQUIST 2876 WAVERLY WAY LIVERMORE CA 94550
2	MARTIN MARIETTA MISSILE SYSTEMS ATTN C E HAMMOND MP 004 L WILLIAMS MP 126 PO BOX 555837 ORLANDO FL 32855-5837
1	BATTELLE ATTN DALE TROTT 505 KING AVE COLUMBUS OH 43201
1	ZERNOW TECH SVCS INC ATTN LOUIS ZERNOW 425 W BONITA AVE SUITE 208 SAN DIMAS CA 91773

NO. OF COPIES	ORGANIZATION
1	OLIN FLINCHBAUGH DIV ATTN RALF CAMPOLI 200 E HIGH ST PO BOX 127 RED LION PA 17356
2	E I DUPONT CO ATTN OSWALD BERGMANN BRIAN SCOTT BRANDYWINE BLDG RM 12204 WILMINGTON DE 19898
1	CHAMBERLAIN MFG CORP ATTN J HEGEDUS 550 ESTER ST PO BOX 2545 WATERLOO IA 50704
1	UNIV OF DAYTON ATTN R HOFFMAN 300 COLLEGE PARK DAYTON OH 45469
3	SIMULA INC ATTN R HUYETT G GRACE G YANIV 10016 S 51ST ST PHOENIX AZ 85044
1	CERADYNE INC ATTN J P MOSKOWITZ 3030 A S RED HILL AVE SANTA ANA CA 92705
1	LANXIDE CORP 1300 MARROWS RD PO BOX 6077 NEWARK DE 19714
2	INST FOR ADV TECH UNIV OF TX AT AUSTIN ATTN H FAIR S BLESS 4030 2 W BRAKER LN AUSTIN TX 78759
1	BRIGGS CO ATTN J BACKOFEN 2668 PETERBOROUGH ST HERNDON VA 22071

NO. OF COPIES	ORGANIZATION
1	SCHWARZKOPF TECH CORP ATTN E KOSINISKI 35 JEFFREY AVE HOLLISTON MA 01746
1	OLIN ORDNANCE ATTN D EDMONDS 10101 9TH ST N ST PETERSBURG FL 33716
1	NEW MEXICO TECH ATTN D EMARY TERA GROUP SOCORRO NM 87801
1	BATTELLE COLUMBUS LABS ATTN DR D TROTT 505 KING AVE COLUMBUS OH 43201
1	RAYTHEON CO ATTN R LLOYD PO BOX 1201 TEWKSBURY MA 01876
1	COORS CERAMICS CO ATTN MR R PARICIO STRUCTURAL DIV 600 NINTH ST GOLDEN CO 80401
1	FMC CORP GROUND SYSTEMS DIV ATTN MR J MORROW 1107 COLEMAN AVE BOX 367 SAN JOSE CA 95103
1	AMERICAN EMBASSY BONN ATTN DR R ROBINSON UNIT 21701 BOX 165 APO AE 09080
1	INGALLS SHIPBUILDING ATTN CBI 01 MR P GREGORY PO BOX 149 PASCAGOULA MS 39567

NO. OF COPIES	ORGANIZATION
2	THE PENN STATE UNIV COLLEGE OF ENGR ATTN DR T KRAUTHAMMER DR R QUNEEY UNIV PARK PA 16802
1	NSWC DAHLGREN DIV G 22 ROWE DAHLGREN VA 22448
15	DIR USARL ATTN AMSRL MA P WOOLSEY J PRIFTI D DANDEKAR S CHOU 10 CPS G BISHOP ATTN SLCMT MRT TECH LIBRARY WATERTOWN MA 02172-0001

NO. OF COPIES	ORGANIZATION
	ABERDEEN PROVING GROUND
46	DIR USARL ATTN AMSRL WT W GILLICH T HAVEL W BRUCHEY S BILYK M BURKINS J DEHN G FILBEY W GOOCH D HACKBARTH G HAUVER E HORWATH G BULMASH Y HUANG M KEELE H MEYER E RAPACKI W ROWE J RUNYEON N RUPERT 10 CP M ZOLTOSKI L MAGNESS K FRANK W DE ROSSET W WALTERS D DIETRICH M LAMPSON S SEGLETES E KENNEDY R KIMSEY T WRIGHT D ECCLESHALL F GRACE 6 CPS

NO. OF COPIES	ORGANIZATION
1	EMBASSY OF AUSTRALIA ATTN DR R L WOODWARD 1601 MASS AVE NW WASH DC 20036-2273

INTENTIONALLY LEFT BLANK.

USER EVALUATION SHEET/CHANGE OF ADDRESS

This Laboratory undertakes a continuing effort to improve the quality of the reports it publishes. Your comments/answers to the items/questions below will aid us in our efforts.

1. ARL Report Number ARL-TR-666 Date of Report January 1995

2. Date Report Received ______

3. Does this report satisfy a need? (Comment on purpose, related project, or other area of interest for which the report will be used.) ______

4. Specifically, how is the report being used? (Information source, design data, procedure, source of ideas, etc.) ______

5. Has the information in this report led to any quantitative savings as far as man-hours or dollars saved, operating costs avoided, or efficiencies achieved, etc? If so, please elaborate. ______

6. General Comments. What do you think should be changed to improve future reports? (Indicate changes to organization, technical content, format, etc.) ______

CURRENT ADDRESS

Organization

Name

Street or P.O. Box No.

City, State, Zip Code

7. If indicating a Change of Address or Address Correction, please provide the Current or Correct address above and the Old or Incorrect address below.

OLD ADDRESS

Organization

Name

Street or P.O. Box No.

City, State, Zip Code

(Remove this sheet, fold as indicated, tape closed, and mail.)

(DO NOT STAPLE)

DEPARTMENT OF THE ARMY

OFFICIAL BUSINESS

BUSINESS REPLY MAIL
FIRST CLASS PERMIT NO 0001, APG, MD

Postage will be paid by addressee

Director
U.S. Army Research Laboratory
ATTN: AMSRL-OP-AP-L
Aberdeen Proving Ground, MD 21005-5066

NO POSTAGE
NECESSARY
IF MAILED
IN THE
UNITED STATES